Available online at www.sciencedirect.com
SCIENCE DIRECT®
Physica E 21 (2004) 204–210
PHYSICA E
www.elsevier.com/locate/physe

Theory of excitons, charged excitons, exciton fine-structure and entangled excitons in self-assembled semiconductor quantum dots

Alex Zunger*, Gabriel Bester

National Renewable Energy Laboratory, 1617 Cole Blvd., Golden, CO 80401, USA

Abstract

We show how the atomistic pseudopotential many-body theory of InGaAs/GaAs addresses some important effects, including (i) the fine-structure splittings (originating from interband spin exchange), (ii) the optical spectra of charged quantum dots and (iii) the degree of entanglement in a quantum dot molecule.

PACS: 71.35.Pq; 73.21.La; 78.67.Hc; 71.10.−w

Keywords: Excitons; Semiconductors; Quantum dots

1. Atomistic theory vs. continuum-like theory of nanostructures

The $k.p$ model [1,2] was eminently successful [3–5] in modeling the electronic structure of three-dimensional (3D) bulk solids and two-dimensional (2D) quantum wells by expanding their wave functions in just a few (1–4), *zone center* (Γ-point) Bloch functions $\phi_{n,\mathbf{k}}(r)$ of the host crystal. In principle, if one were to use a complete basis, this method would be exact. However, this is not practical, since in this empirical approach the number of adjustable parameters of the theory increases rapidly with the number of basis functions. Moreover, many of these $k.p$ parameters are not direct physical observables, so they cannot be measured, even in principle. Thus, whereas conventional basis-set expansion methods (e.g., plane-wave pseudopotentials or LAPW for solids) routinely increase their basis sets until convergence is demonstrated, the standard $k.p$ model relies instead on a fixed and rather small number of basis orbitals, using adjustable parameters to mitigate variational (basis set) limitations. This works well for 3D bulk or 2D wells, but not for 0D dots. This was demonstrated by projecting realistically calculated (i.e., not $k.p$) wave functions of 0D dots on 3D bulk Bloch function basis [6–11], showing that $\simeq 100$ bulk Γ bands are often needed for a realistic expansion of 0D wave functions. Hence, one cannot expect accurate results assuming just 1–4 $k.p$ states. One may still hope, however, that even though such a large number of basis functions is needed in principle, in practice one may be able to re-adjust the free parameters of the small basis set theory to match experiment. But one thing is difficult to fix by reparametrization: the correct symmetry of the object being modeled. If one has just a small number of Bloch functions, the broad

* Corresponding author.
E-mail address: azunger@nrel.gov (A. Zunger).

1386-9477/$ - see front matter © 2003 Elsevier B.V. All rights reserved.
doi:10.1016/j.physe.2003.11.156

and featureless envelope functions $F_n(\boldsymbol{r})$ cannot properly resolve the atomistic detail of the object being modeled. Thus, the theory is "hyperopic", seeing the global shape but not the detailed symmetry. This was demonstrated recently in Ref. [12], where $k.p$ was shown to miss the correct symmetry of dots, leading to gross errors in predicting optical properties.

The alternative approach is to use an *atomistic* theory, in which the potential $\sum_\alpha \sum_n v_\alpha(\boldsymbol{r}-\boldsymbol{R}_n)$ is modeled by superposing (screened) atomic potentials v of type α at site $\boldsymbol{R}_n$, and the wave function is expanded in a basis capable of resolving atomistic details. This is provided by our empirical plane-wave pseudopotential method [13], where the single-particle wave functions $\psi(\boldsymbol{r})$ are expanded in terms of strain-dependent Bloch functions $\phi_{n,\boldsymbol{k}}(r)$:

$$\psi(\boldsymbol{r}) = \sum_{n}^{N_B} \sum_{k}^{N_k} C_{\boldsymbol{k},n}\phi_{\boldsymbol{k},n}(\boldsymbol{r}) \tag{1}$$

with band index n and wave vector $\boldsymbol{k}$ of the underlying bulk solids ("Strain dependent Linear Combination of Bulk Bands" (SLCBB) [13]). The method naturally includes the effect of strain, alloy fluctuations, composition gradients and spin–orbit interaction. In the next step we follow the configuration interaction (CI) method and construct a set of Slater determinants $|\Phi_{h_i,e_j}\rangle$ from the antisymmetrized product of the single-particle wave functions ψ_i [14]. The exciton wave functions $|\Psi\rangle$ are expanded in terms of this determinantal basis set:

$$|\Psi\rangle = \sum_{h_i,e_j} A(h_i,e_j)|\Phi_{h_i,e_j}\rangle. \tag{2}$$

Here we illustrate the method for three cases: The calculation of the fine-structure, the charged exciton spectra and the degree of entanglement in self-assembled quantum dots.

2. The excitonic fine-structure of InGaAs/GaAs quantum dots

Fig. 1 shows how the normal excitonic structure (top panel) is resolved, at high resolution, into fine-structure (lower panel). Each exciton is split into 4 levels that we denote as 1, 2, 3 and 4 in increasing order of energy. The splitting between the levels 1 and 2 is generally very small and is due to mixing of valence band $|z\rangle$ character into the hole states [15]. This mixing increases with increasing dot height. The splitting between the states 2 and 3 is the singlet–triplet splitting due to electron–hole exchange interaction which is also present in dots with cylindrical symmetry. The splitting between the states 3 and 4 is the most interesting splitting: It is obtained when both the true atomistic symmetry of the quantum dot and the spin–orbit interaction are taken into account. The bright states 3 and 4 can be resolved experimentally and are polarized (see Ref. [15]). We predicted [15] the fine-structure splitting for an InAs dot (Fig. 1), an alloyed $In_{0.6}Ga_{0.4}As$ lens-shaped dot ($b = 25.2$ nm, $h = 3.5$ nm), a taller $In_{0.6}Ga_{0.4}As$ lens-shaped dot ($b=25.2$ nm, $h=5$ nm), and an elongated $In_{0.6}Ga_{0.4}As$ (elliptical base with $b1 = 26$ nm, $b2 = 20$ nm and $h = 3.5$ nm) dot. The splitting Δ_{3-4} of the bright states shows as an overall trend a larger splittings for transitions of the P–P and D–D channels (9–46 μeV) than exhibited in the S–S channel (2–30 μeV). The weak, "forbidden" e_S–h_P transition exhibit a surprisingly large (166 μeV) splitting. Asymmetries in the overall dot shape (elongated dot) tend to increase the splittings. Notably, even cylindrically-symmetric dots have non-zero splittings. Experimentally, δ is between 0–150 μeV [16,17] for the ground state exciton. A value as large as 150 μeV is not predicted for the present dots, but is nevertheless conceivable for strongly elongated tall dots. The singlet–triplet splitting Δ_{2-3} are in very good agreement with the experiment. Bayer et al. [17] measure for the ground states exciton $\Delta_{2-3} = 116$ μeV for a dot of approximately 25 nm diameter. This value agrees very well with the calculated 107 μeV for our tallest dot. Furthermore, we report larger values for Δ_{2-3} in strongly confined systems like in the elongated dot (20 nm confinement in the x–y plane) and in the pure InAs dot (larger band-offsets). This trend has also been observed experimentally (Fig. 7 in Ref. [17]). The splitting Δ_{1-2} of the "dark" states are small (< 4 μeV) for all the considered dots. The bright states show strong polarization in [1 1 0] and [$\bar{1}$ 1 0] directions. Even for circular-based lens-shaped dots we predict 100% polarization and show that measurements of finite polarizations cannot be used as evidence for dot shape anisotropies [15].

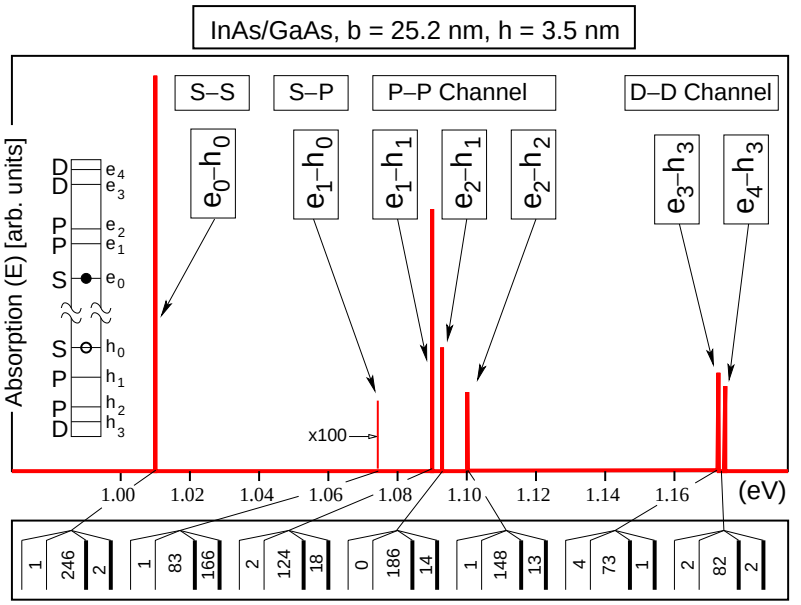

Fig. 1. Absorption spectra for a pure lens-shaped (base = 25.2 nm, height = 3.5 nm) InAs dot. Upper panel: low-resolution excitonic structure (CI with Coulomb only). Lower panel: fine-structure splittings (CI with both Coulomb and exchange) in μeV. Thin (heavy) lines denote dark (bright) states.

3. Charged excitons in InGaAs/GaAs quantum dots

Fig. 2 shows the calculated photoluminescence of both negatively and positively charged dots. We consider here a lens-shaped $In_xGa_{1-x}As$ dot (base $(b) =$ 20 nm, height $(h) = 5$ nm) with an onion-like composition profile with x reaching from 0.8 in the core to 0.2 at the outer boundary of the dot. This choice for this size and composition profile is inspired from the experiments of Walther et al. [18] and Kegel et al. [19]. All calculated dots are embedded in GaAs and have one monolayer thick InGaAs wetting layer. Fig. 3 shows the relative shifts of the main X^0, $X^{-/+}$ and $X^{2-/2+}$ peaks (as defined in the caption) as a function of the In composition x and the height of the dot h. The main features of the calculated spectra are:

(i) The shifts A^+ vs. A^- as well as B^+ vs. B^- show opposite trends as function of the composition and height: A^+ and B^+ increase with increasing In composition and height, while A^- and B^- decrease with x and h. There is a crossover of (A^+, A^-) and (B^+, B^-) at $\approx 80\%$ In and at ≈ 4.6 nm dot height.

(ii) The excitonic structure of the negatively charged onion dot in Fig. 2 presents some striking peak symmetries and alignments: the X^- and X_a^{2-} transitions are aligned; the main peak of X^{3-} is located midway between the X_a^{2-} and the X_b^{2-} transitions and is aligned with the X_a^{4-} peak.

(iii) Three transitions are observed in the X^{3-} spectrum in Fig. 2, in contradiction with previous models which start from degenerate electron P-states and predict two peaks [20–25]. In Ref. [26] the authors expect either two or one peak depending on the splitting of the electron P-states [26].

We have explained [27] the effects (i) and (ii) in terms of a crossover in the localization of electron and hole wave functions. Correlations are shown to qualitatively change the conclusions. Effect (iii) is related to a detailed balance between exchange interaction and the splitting of the single particle energy of the electron P-states [27].

To compare with experiment we selected two dots that have a composition and shape close to the one suggested in the literature [18,19,26]: the onion dot and a lens-shaped $In_{0.6}Ga_{0.4}As$ dot ($b = 20$ nm, $h =$

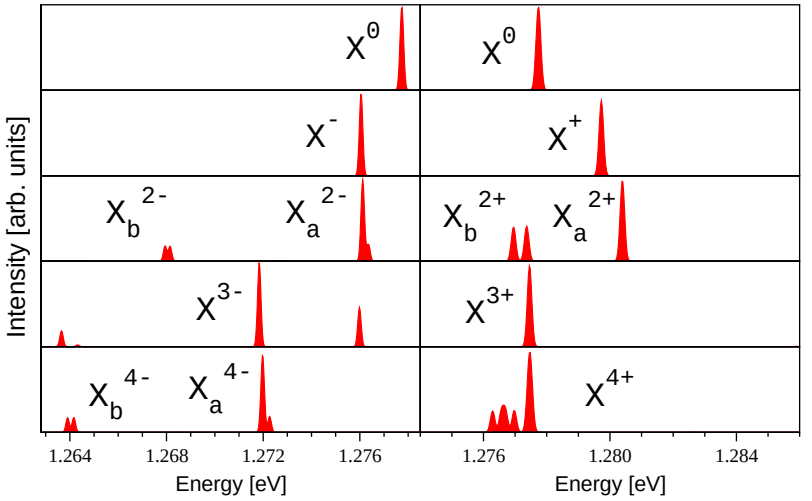

Fig. 2. Calculated PL spectra for different charged states of a lens-shaped $In_xGa_{1-x}As$ dot (base $(b) = 20$ nm, height $(h) = 5$ nm) with an onion-like composition profile with x reaching from 0.8 in the core to 0.2 at the outer boundary of the dot.

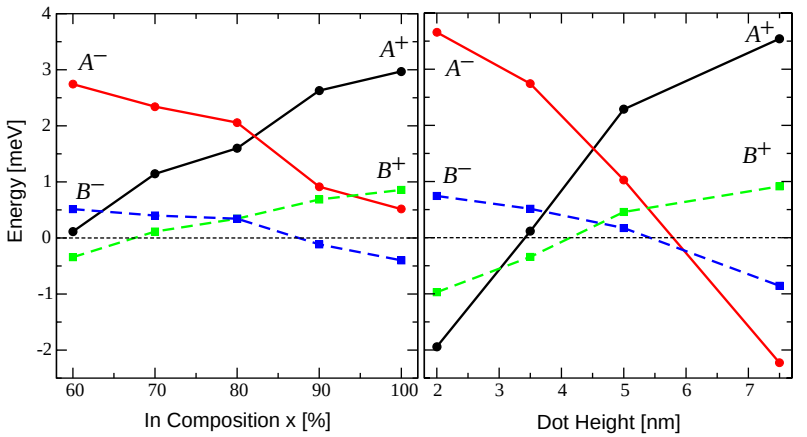

Fig. 3. Spectroscopic shifts $A^+ = X^0 - X^+$, $A^- = X^0 - X^-$ (both solid lines), $B^+ = X^+ - X_a^{2+}$, $B^- = X^- - X_a^{2-}$ (both dashed lines) as a function of composition (for a lens-shaped dot of base 25 nm and height 3.5 nm) and height (for an $In_{0.6}Ga_{0.4}As$ lens-shaped dot with 25 nm base).

Table 1
Compilation of the available experimental results on spectroscopic shift in $In_xGa_{1-x}As/GaAs$ quantum dots

	A^-	A^+	B^-	C^-
Exp. [26,29–32,34,35]	3.1–5.8	−0.8–−1.5	0.0–0.5	4.1–4.9
Calc. onion	1.7	−2.0	0.2	8.1
Calc. $In_{0.6}Ga_{0.4}As$ $h = 2$ nm, $b = 25$ nm	3.7	−1.9	0.7	7.7

5 nm). The results are compared with experiment in Table 1. The measured [22,26,28–36] red shift A^- and the blue shift [28,35] A^+ agree very well with our calculation. Also the calculated alignment of the X^- and X_a^{2-} transitions (small values of B^-) is in excellent agreement with Refs. [26,28–31,36] and the fact that the X^{3-} transition is located midway between the X_a^{2-} and X_b^{2-} transitions is also observed experimentally in Ref. [26,28]. The exchange splitting C^- on the other hand tends to be overestimated by the theory. This might be attributed to shape anisotropy effects. The calculated excitonic dipole moment for the onion dot (7.2×10^{-29} cm) agrees well with the measured dipole of Fry et al. [37] ($(7 \pm 2) \times 10^{-29}$ cm and Findeis et al. [30] (8) $\times 10^{-29}$ cm where in all cases the holes are above the electrons.

4. Entanglement in dot molecules

Fig. 4 shows the single-particle and many-particle energies of a dot molecule vs. distance, as obtained by Bayer et al. in a "simple model", and in our atomistic calculations. Bayer et al. [38] offered a simple model to evaluate the energies of these four excitonic states, and compared them with experiment. In their model it was assumed that the two dots, T (top) and B (bottom) forming the molecule have identical on-site single-particle ("tight-binding") energies $\varepsilon_T = \varepsilon_B$ that do not depend on inter-dot separation. They also assume identical hoping matrix elements for electrons and holes, $t_e = t_h$. Under these assumptions, the single-particle molecular orbital energies split *symmetrically* as a function of inter-dot distance (much like a homo-nuclear diatomic molecule), as shown in Fig. 4(a). This model leads to the two-particle states $|1\rangle$, $|2\rangle$, $|3\rangle$ and $|4\rangle$ shown in Fig. 4(b), with wave functions illustrated schematically on the right-hand side of Fig. 5. The optically allowed exciton states $|1\rangle$ and $|3\rangle$ start at large inter-dot separation as pure $|a\rangle$ and pure $|b\rangle$ states, respectively, having thus equal excitonic amplitude on the two dots, and showing maximum entanglement. As the inter-dot separation diminishes, excitons $|1\rangle$ and $|3\rangle$ couple via the hoping matrix elements t_e and t_h and become linear combinations of the bonding excitons, $|a\rangle$ and $|b\rangle$.

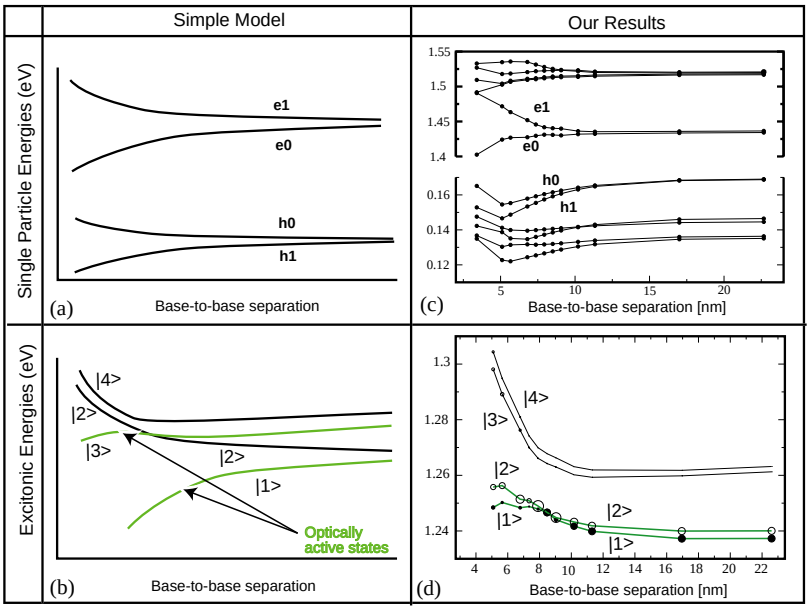

Fig. 4. Calculated results for single-particle energies (a and c) and excitonic energies (b and d) of the model of Bayer et al. [38] (a and b) and the present pseudopotential CI calculation (c and d). The circles on the excitonic lines of panel (d) are proportional to the oscillator strength of the transition.

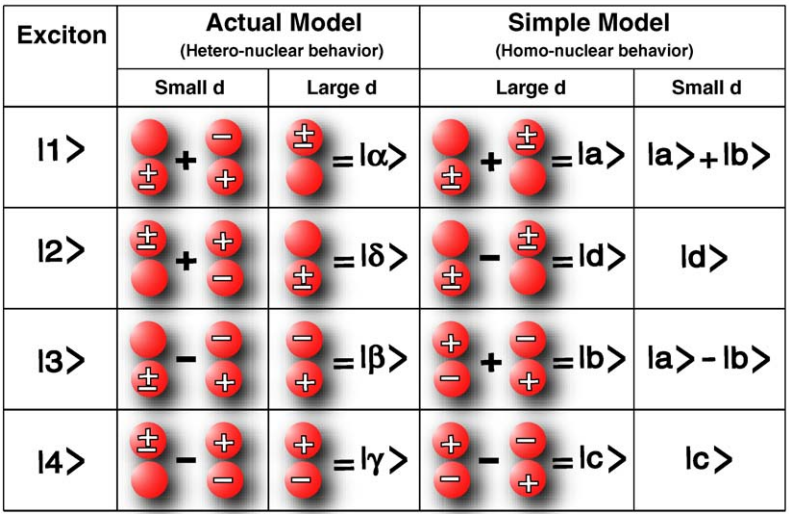

Fig. 5. Schematic representation of the excitonic wave functions obtained in our model (left), and in the simple model of Bayer et al. [38] (right). The symbols are: +(hole), −(electron) or ±(exciton). The two spheres denote top and bottom dots.

The excitonic spectra we calculated for our dot molecules are shown in Fig. 4(d) and is very different from the simple model. Our dots are 12 nm × 2 nm truncated-cone-shaped dots, with a linear composition gradient varying from $In_{0.5}Ga_{0.5}As$ at their bases to pure InAs at their tops. In Fig. 4(d) the oscillator strength of the first four excitons $|1\rangle$, $|2\rangle$, $|3\rangle$ and $|4\rangle$ is proportional to the size of the circles. We see (i) at large inter-dot separations only the first two excitons $|1\rangle$ and $|2\rangle$ are optically allowed, corresponding to excitons where the electron–hole pair is localized to the top and bottom dot, respectively. In contrast, the excitons $|1\rangle$ and $|3\rangle$ are optically allowed in the simple model. The dots are geometrically identical but due to random alloy fluctuations present in real dots, and taken into account in our calculations, the top dot is preferred by the exciton (see Fig. 5). The "dissociated states" $|3\rangle$ and $|4\rangle$, where the electron and the hole resides on different dots have no oscillator strength since there is no e–h overlap. (ii) At small inter-dot separation there are four states, all dipole-allowed. This is due to the interaction of the four excitons $|1\rangle$, $|2\rangle$, $|3\rangle$ and $|4\rangle$ which mix, like shown in Fig. 5. All four excitons are mixed excitonic-dissociated states with non-zero oscillator strength. (iii) At large inter-dot separation, the exciton states $|1\rangle$ and $|2\rangle$ and the dissociated states $|3\rangle$ and $|4\rangle$ are separated by about 20 meV.

(iv) The lines collapse into one at a special separation of 8.5 nm. At this separation the entanglement (that can be calculated from our CI wave functions, following the definition of Von Neumann [39,40]) reaches a maximum of 80%. The degree of entanglement sharply drops for larger and shorter inter-dot separations (not shown).

References

[1] E. Kane, J. Phys. Chem. Sol. 1 (1957) 249.
[2] J. Luttinger, W. Kohn, Phys. Rev 97 (1955) 869.
[3] G. Baraff, D. Gershoni, Phys. Rev. B 43 (1991) 4011.
[4] G. Bastard, Wave Mechanics Applied to Semiconductor Heterostructures, Halstead, New York, 1988.
[5] M. Cardona, F. Pollak, Phys. Rev 142 (1966) 530.
[6] A. Franceschetti, S. Wei, A. Zunger, Phys. Rev. B 50 (1994) 8094.
[7] A. Franceschetti, S. Wei, A. Zunger, Phys. Rev. B 52 (1995) 13992.
[8] H. Fu, L. Wang, A. Zunger, Phys. Rev. B 57 (1998) 9971.
[9] H. Fu, L. Wang, A. Zunger, Appl. Phys. Lett. 73 (1998) 1157.
[10] L. Wang, A. Zunger, Phys. Rev. B 54 (1996) 11417.
[11] D. Wood, A. Zunger, Phys. Rev. B 53 (1996) 7949.
[12] A. Zunger, Phys. Stat. Sol. (A) 190 (2002) 467.

[13] L.-W. Wang, A. Zunger, Phys. Rev. B 59 (1999) 15806.
[14] A. Franceschetti, et al., Phys. Rev. B 60 (1999) 1819.
[15] G. Bester, S.V. Nair, A. Zunger, Phys. Rev. B 67 (2003) 161306.
[16] M. Bayer, et al., Phys. Rev. Lett. 82 (1999) 1748.
[17] M. Bayer, et al., Phys. Rev. B 65 (2002) 195315.
[18] T. Walther, et al., Phys. Rev. Lett. 86 (2001) 2381.
[19] R. Kegel, P.M. Petroff, et al., Phys. Rev. B 63 (2001) 035318.
[20] Y. Ducommun, et al., Phys. Stat. Sol. (B) 224 (2001) 325.
[21] U. Hohenester, E. Molinari, Phys. Stat. Sol. (B) 221 (2000) 19.
[22] D.V. Regelman, et al., Physica E 13 (2002) 114.
[23] R.J. Warburton, et al., Phys. Rev. B 58 (1998) 16221.
[24] R.J. Warburton, et al., Nature 405 (2000) 926.
[25] R.J. Warburton, et al., Physica E 9 (2001) 124.
[26] J.J. Finley, et al., Phys. Rev. B 63 (2001) 161305.
[27] G. Bester, A. Zunger, Phys. Rev. B 68 (2003) 073309.
[28] A. Ashmore, et al., Physica E 13 (2002) 127.
[29] M. Baier, et al., Phys. Rev. B 64 (2001) 195326.
[30] F. Findeis, et al., Appl. Phys. Lett. 78 (2001) 2958.
[31] F. Findeis, et al., Phys. Rev. B 63 (2001) 121309.
[32] A. Hartmann, et al., Phys. Rev. Lett. 84 (2000) 5648.
[33] K. Karlsson, E. Moskalenko, P. Holtz, B. Monemar, W. Schoenfeld, J. Garcia, P. Petroff, Physica E 13 (2002) 101.
[34] K.F. Karlsson, et al., Acta. Phys. Pol. 100 (2001) 387.
[35] D.V. Regelman, et al., Phys. Rev. B 64 (2001) 165301.
[36] A. Zrenner, et al., Physica E 13 (2002) 95.
[37] P.W. Fry, et al., Phys. Rev. Lett. 84 (2000) 733.
[38] M. Bayer, et al., Science 291 (2001) 451.
[39] C.H. Bennett, D.P. DiVincenzo, Nature 404 (2000) 247.
[40] M.A. Nielsen, I.L. Chuang, Quantum Computation and Quantum Information, Cambridge University Press, Cambridge, 2000.